J. Univ. Kuwait (Sci.) **6**, 1979

Petrography and mineralogy of some andesite dykes, Abu Dob area, Eastern Desert, Egypt

AHMED M. BISHADY*, MOHAMED E. HILMY† AND MAHMOUD L. KABESH‡

**Teachers' Institute of Education, El-Odylia, Kuwait; †Department of Geology, Faculty of Science, Ain Shams University, Cairo, Egypt, ‡Earth Sciences Laboratory, National Research Centre, Dokki, Cairo, Egypt*

ABSTRACT

Andesite dykes dissecting the granitic complex of Gebel Abu Dob, Eastern Desert, Egypt are studied. Thin section examination revealed several petrographic varieties comprising: plagioclase-hornblende andesite prophyry, porphyritic plagioclase-biotite-hornblende andesite, porphyritic quartz-andesite, plagioclase-hornblende andesite, and pyroxene-hornblende andesite. X-ray measurements of plagioclase separated from six porphyritic andesites revealed that it is of moderately ordered structural state.

INTRODUCTION

The present study deals with some andesite dykes dissecting the granitic complex of Gebel Abu Dob, Eastern Desert, Egypt (Fig. 1). The pluton of Abu Dob is formed mainly of granites dissected by scores of post-granitic dykes of acidic, intermediate, basic, and alkaline composition. The dominant trend of these dykes is either NS or NE–SW. They tend to form swarms, which are vertical or steeply inclined (Salem 1972). Most of the examined dykes are fairly straight indicating their possible emplacement along defined fissures.

PETROGRAPHY

Two main textural types are recognized among these andesite dykes: even-grained (non-porphyritic) and porphyritic. The majority are almost holocrystalline and in few cases hyalopilitic. Difference in texture among the examined andesite dykes may be explained in the light of the argument presented by Rittmann (1962), who indicated that the texture of a solidified volcanic rock is determined by the viscosity and the degree of crystallisation of the melt at the moment of its intrusion as well as by its subsequent rates of cooling.

Generally, megacrysts in the examined porphyritic andesite and andesite porphyry dykes are represented by plagioclase, hornblende and biotite; the plagioclase megacrysts are dominant. Trachytic and subtrachytic textures are less common. Micro-

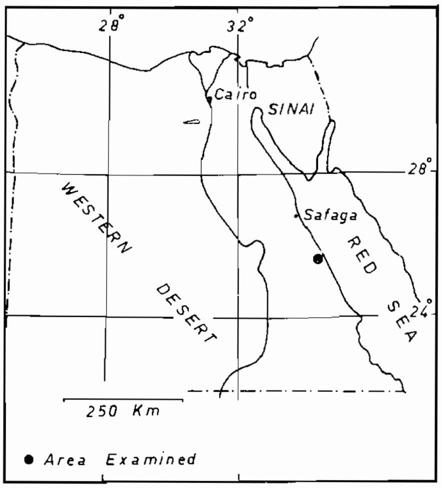

Fig. 1. Location map.

scopic examination of the andesite dykes revealed several varieties which comprise: plagioclase-hornblende andesite porphyry, porphyritic plagioclase-biotite-hornblende andesite, porphyritic quartz andesite, plagioclase-hornblende andesite and pyroxene-hornblende andesite.

Plagioclase occurs in all the examined andesite dykes; it is present as megacrysts and as smaller crystals approaching groundmass dimensions down to microlites recognisable under the microscope. Plagioclase megacrysts vary in length from 3 to 3·5 mm and in breadth from 1·5 to 3 mm. Plagioclase of the groundmass varies in length from 0·1 to 0·8 mm and in breadth from 0·05 to 0·35 mm. Plagioclase megacrysts may exhibit irregular fractures cutting across the twinning planes. The origin of these fractures was discussed by Goodspeed (1959) and may be attributed to: (1) The crystal mesh of the cooling magma may have been subjected to a uniform internal stress which was resisted by the feldspars. (2) Some of the plagioclase megacrysts may have been of intratelluric origin and thus formed under conditions of high pressure. The sudden diminution of this pressure as the crystals move upward might result in their expansion, thus producing fractures. Such fractures played an important role in the final stages of crystallisation of the andesites in that they create minute paths for late magmatic and deuteric alterations. However, it is noticed that these fractures may be filled with chlorite and iron oxides. Corroded plagioclase megacrysts of the andesites examined may exhibit well-defined ragged irregular and embayed outlines. Such outlines are apparently due to magmatic corrosion.

The composition of the plagioclase tends to be calcic. The average composition of the megacrysts is about An_{55}. However, some megacrysts may be as calcic as An_{60}. The composition of the plagioclase in the groundmass is about An_{46} to An_{50}. It is worthy of mention that although the plagioclase feldspars occur in more than one generation, the variation in composition between the megacrysts and those of the groundmass is so small that a sharp line cannot be demarcated between them.

Hornblende is present as megacrysts and in the groundmass. Hornblende megacrysts vary in length from 0·8 to 1·7 mm and in breadth from 0·5 to 0·9 mm. In the groundmass it attains up to 0·5 mm in length and 0·2 mm in breadth. The green variety is more common among the megacrysts while the brown variety is rather dominant in the groundmass. In megacrysts $z \wedge c$ ranges from $-10°$ to $-13°$ while in hornblende of the groundmass it ranges from $-15°$ to $-19°$. Hornblende megacrysts are subhedral, occasionally simply twinned. They are rimmed by a jacket of iron oxides and occasionally the hornblende has been completely replaced by chlorite. The hornblende andesites of Abu Dob are rich in hornblende and lack pyroxenes.

Biotite is quite common only in the groundmass. It forms anhedral flakes ranging from 0·4 to 2·5 mm in length and 0·2 to 1·5 mm in breadth. It may form aggregated flakes which are mostly chloritised. Inclusions in biotite are common and comprise zircon, apatite and magnetite. In few cases biotite is present as an alteration product of hornblende.

Pyroxenes are uncommon and are represented by hypersthene and diopsidic augite. Hypersthene occurs as small anhedral crystals attaining up to 1·8 mm in length and 1·1 mm in breadth. Diopsidic augite is less common than hypersthene and occurs as subhedral crystals in the groundmass, attaining up to 0·3 mm in length and 0·2 mm in breadth.

Accessories are represented by iron oxides as magnetite occurring as subhedral grains about 0·2 mm across, but limonite is also observed. Clear subrounded quartz reaching up to 0·3 mm across as well as apatite are also observed as accessories. Glass is recognized in some of the examined andesites.

Some of these andesites are intensely altered to deserve the term propylite. These rocks are formed of strongly decomposed plagioclase, chloritized hornblende and biotite. Lamellar twinning and crystal boundaries of the plagioclase are completely obliterated, and the crystals are full of granular epidote and carbonates. Hornblende may be completely pseudomorphed by chlorite. The groundmass contains fair amounts of iron oxides as dust and grains.

Modal composition. Twenty-three andesite samples were point-counted (Table 1). Six classes, namely plagioclase, hornblende, biotite, pyroxene, accessories and alteration products were counted. In the porphyritic andesites the volume percentages of the megacrysts have been counted. The sum of the volume percents of the megacrysts and the groundmass represents the total area counted. From the modal composition it is evident that megacrysts in the examined porphyritic andesites and andesite porphyries show a wide range from 1·39% up to 24·85%. Plagioclase megacrysts representing the dominant megacrystic constituents vary between 1·39% and 24·85%. Hornblende megacrysts do not show a wide range as they vary from 1·58% to 6·84%.

Colour index. With respect to the examined andesite dykes of Abu Dob area, the colour index is taken to represent the percentage of coloured minerals (hornblende + biotite + pyroxene), accessories and alteration products. The colour index of the examined andesite dykes (Table 1) is somewhat high and ranges from 32·3% to 63·8% with an average of 40·1%. The andesite dykes are considered mesocratic according to the classification of Streckeisen (1967).

X-RAY MINERALOGY

Plagioclase separated from six porphyritic andesites was investigated using the X-ray powder diffraction (Tables 2–7). Γ and β functions of Smith & Gay (1958) are considered here (Table 8) as the most appropriate functions which indicate the special

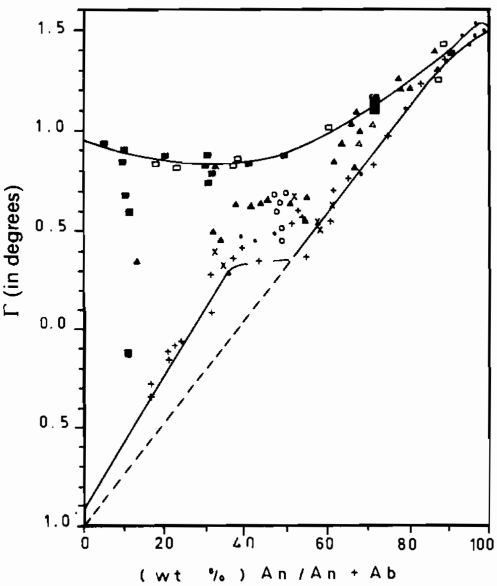

Fig. 2. The variation of Γ function and An content of plagioclases (curve after Smith & Gay 1958). o, Represents the plagioclases in the andesites of present work. The symbols used by Smith and Gay (1958) for plagioclases are: ■, synthetic; □, heated natural; ▲, volcanic; △, hypabyssal; +, plutonic and pegmatitic; ×, metamophic and charnockitic; ●, Skaergaard, Stillwater and Bushveld igneous complexes.

angular separation due to variation in the structural state or An content of plagioclases, within the range of An_{20} to An_{70} (Smith 1974).

The structural state here is an indication of the thermal conditions which prevailed through the rock solidification, although the temperature recorded by that thermometer could be much lower than the highest temperature to which the rock was exposed (Barth 1962).

Smith & Gay (1958) gave two series of plagioclase structures, the 'high series'

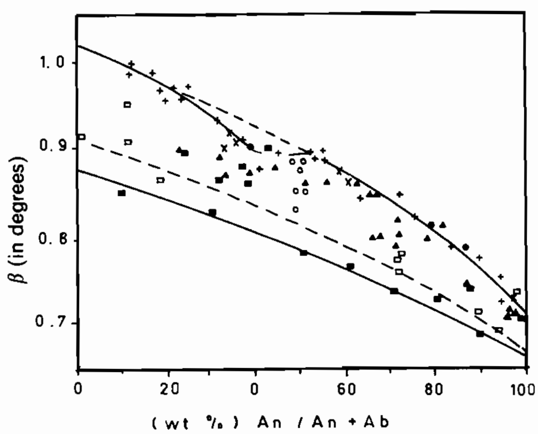

Fig. 3. The variation of β function and An content of plagioclases (curve after Smith & Gay 1958). o, Represents the plagioclases in the andesites of present work. The symbols used by Smith & Gay (1958) for plagioclases are: ■, synthetic; □, heated natural; ▲, volcanic; △, hypabyssal; +, plutonic and pegmatitic; ×, metamorphic and charnockitic; ●, Skaergaard, Stillwater and Bushveld igneous complexes.

corresponding to the most disordered series, that is, the rapidly cooled rocks, and the 'low series' corresponding to the structures with the highest degree of order and thus smooth cooling. The Γ function of Smith & Gay (1958) obtained mainly from the measurements of reflections depends on angle γ and is expressed in the angle $2\theta(131)+2\theta(220)-4\theta(1\bar{3}1)$. The β separation angle (*sensu* Smith & Gay 1958) $2\theta(111)-2\theta(\bar{2}01)$ depends largely on the crystallographic angle β.

Figs. 2 and 3 show the plotting of Γ and β separation calculated in the present work from the X-ray diffraction patterns and provided that the plagioclase in megacrysts and groundmass has an average composition of approximately An_{50}. The figures show a complete accordance with the intermediate or relatively low series of Smith and Gay (1958). The separation values match with those of the intermediate ordering of the hypabyssal rock group (M group) of the same authors (Smith & Gay 1958, Table 1, p. 75). Such measured values are in harmony with the petrographic characters of plagioclases mentioned above.

REFERENCES

Barth, T.F.W. 1962. The feldspar geologic thermometers. Norsk. Geol. Tidesk. **42:**330–9.

Goodspeed, G.E. 1959. Some textural features of magmatic and metasomatic rocks. Amer. Mineral. **44:** 211–50.

Rittmann, A. 1962. Volcanoes and their activity. John Wiley and Sons, New York.

Salem, A.K.A. 1972. Geological and geochemical studies on Gebel Abu Dob Area, Eastern Desert. M.Sc. Thesis, Fac. Sci., Ain Shams University, Cairo, Egypt.

Smith, J.V. 1974. Feldspar minerals, vol. 1. Springer Verlag, Berlin.

Smith, J.V. & Gay, P. 1958. The powder patterns and lattice parameters of plagioclase feldspars. II. Mineral. Mag. **31:** 744–62.

Streckeisen, A. 1967. Classification and nomenclature of igneous rocks. N. Jb. Miner. Abh. **107:** 144–214.

(Received 8 October 1977)

Table 1. Modal analysis of andesite dykes.

Sample no.	1	2	3	4	5	6	7	8	9	10	11	12	13	14	15	16	17	18	19	20	21	22	23
Megacrysts																							
Plagioclase	13·1		15·4	12·7	5·7	8·3	13·1	20·7		16·9	24·8				2·7	1·4		15·0	6·3	7·7		3·4	
Hornblende	2·5			4·6	1·6	6·8	3·5			2·9									5·7	1·4			5·1
Groundmass																							
Plagioclase	33·5	47·1	49·1	39·6	52·6	34·7	35·9	40·1	47·7	36·3	31·0	56·3	36·2	60·2	55·1	55·8	53·4	50·3	50·1	45·7	49·9	37·3	47·8
Hornblende	17·1	6·4	18·9	22·8	16·1	24·4	14·7	17·7	14·3	13·6	21·5	29·2	43·4	9·9	19·4	20·5	30·8	20·9	20·1	15·4	20·5	32·2	21·3
Biotite	1·3	6·8		1·4						3·3				3·8				2·8		1·1			
Quartz	2·4		2·6	5·2	7·9	2·5	6·0	5·8		1·7	5·1				8·0	10·5	9·7		8·4	9·9	11·8		8·9
Accessories	19·4	16·4	8·3	10·5	10·1	13·8	16·5	6·8	15·3	13·4	9·2	9·1	18·8	20·6	7·3	9·0	5·0	6·8	5·3	10·9	8·0	8·5	9·0
Alteration products	10·7	23·3	5·7	3·2	6·1	9·5	10·3	8·9	22·7	11·9	8·4	5·4	1·6	5·5	7·6	2·8	1·1	4·2	4·1	7·9	9·8	18·6	7·9
Total	100	100	100	100	100	100	100	100	100	100	100	100	100	100	100	100	100	100	100	100	100	100	100
Color index	51·0	52·9	32·9	42·5	33·9	54·5	45·0	33·4	52·3	45·1	39·1	43·7	63·8	39·8	34·3	32·3	36·9	34·7	35·2	36·7	38·3	59·3	43·3

Table 2. X-ray diffraction data of the light fraction of Sample No. 1.

2θ	dA°	I/Io	hKL	Corresponding mineral phase
20·25	4·386	13·98		Quartz
20·82	4·266	15·05		Quartz
21·10	4·210	17·20		Nepheline
21·35	4·162	12·90		Plagioclase
22·15	4·014	17·74	$\bar{2}01$	Plagioclase
22·25	3·997	17·20		Plagioclase
22·56	3·940	13·98		Plagioclase
23·03	3·960	12·90	$1\bar{1}1$	Plagioclase
23·28	3·821	16·13		Plagioclase
23·67	3·757	22·58		Plagioclase
24·27	3·666	25·80		Plagioclase
24·90	3·576	12·90		Plagioclase
25·86	3·445	15·05		Plagioclase
26·40	3·376	12·90		Plagioclase
26·65	3·344	48·38		Plagioclase
27·35	3·262	32·25		Plagioclase
27·62	3·227	72·03		Plagioclase
28·07	3·180	100·00		Plagioclase
28·90	3·089	15·05		Plagioclase
29·00	3·077	13·95	220	Plagioclase
29·73	3·005	17·20		Plagioclase
30·10	2·968	18·20	$1\bar{3}1$	Plagioclase
30·40	2·941	19·30		Plagioclase
31·45	2·843	16·13		Plagioclase
31·70	2·820	16·13	131	Plagioclase
32·27	2·775	12·90		Analcite
32·85	2·722	17·20		Analcite

Table 3. X-ray diffraction data of the light fraction of Sample no. 2

2θ	dA°	I/Io	hKL	Corresponding mineral phase
21·20	4·191	24·66		Plagioclase
21·75	4·085	19·18		Plagioclase
21·95	4·050	26·72	$\bar{2}01$	Plagioclase
22·15	4·014	26·03		Plagioclase
22·78	3·895	22·19	$1\bar{1}1$	Plagioclase
23·42	3·798	24·66		Plagioclase
23·60	3·770	28·77		Plagioclase
23·85	3·730	24·66		Plagioclase
24·25	3·670	25·35		Analcite
25·20	3·534	34·25		Analcite
26·15	3·409	23·98		Plagioclase–Analcite
26·65	3·345	43·16		Plagioclase
27·67	3·224	47·95		Plagioclase
28·00	3·187	100·00		Plagioclase
28·35	3·148	41·10	220	Plagioclase
28·87	3·089	26·03		Analcite
29·15	3·063	21·92		Plagioclase–Analcite
29·65	3·013	23·29	$1\bar{3}1$	Plagioclase
29·96	2·982	23·98		Plagioclase
30·40	2·940	28·77		Plagioclase
30·59	2·922	28·09		Analcite–Plagioclase
30·90	2·894	23·29		Plagioclase
31·40	2·849	21·92	131	Plagioclase
31·92	2·804	26·03		Analcite
32·62	2·745	24·66		Analcite
33·15	2·703	26·03		Analcite

Table 4. X-ray diffraction data of the light fraction of Sample no. 3

2θ	dA°	I/Io	hKL	Corresponding mineral phase
20·37	4·357	37·22		Quartz
22·12	4·019	45·36	$\bar{2}01$	Plagioclase
22·35	3·977	37·22		Plagioclase
23·00	3·865	37·22	$1\bar{1}1$	Plagioclase
23·65	3·760	44·19		Plagioclase
24·00	3·706	43·03		Plagioclase
24·40	3·637	40·71		Plagioclase–Analcite
24·90	3·575	39·54		Plagioclase–Analcite
25·10	3·547	53·50		Plagioclase
25·70	3·466	45·36		Plagioclase–Analcite
26·10	3·415	43·03		Plagioclase–Analcite
26·65	3·345	40·71		Plagioclase–Analcite
26·85	3·320	46·52		Plagioclase
27·17	3·283	51·17		Plagioclase
27·70	3·220	72·11		Plagioclase
27·90	2·198	100·00		Plagioclase
28·70	3·110	74·43	220	Plagioclase
29·00	3·077	41·87		Plagioclase
29·83	2·995	46·52	$1\bar{3}1$	Plagioclase
30·10	2·968	44·66		Plagioclase
30·40	2·941	39·54		Plagioclase
30·70	2·912	37·22		Plagioclase–Analcite
31·10	2·873	39·54		Analcite
31·60	2·831	44·19	131	Plagioclase
32·15	2·784	41·87		Analcite
32·50	2·755	45·36		Analcite

Table 5. X-ray diffraction data of the light fraction of Sample no. 4

2θ	dA°	I/Io	hKL	Corresponding mineral phase
20·65	4·302	15·68		Quartz
20·95	4·240	17·64		Plagioclase
21·93	4·046	15·68		Plagioclase
22·10	4·023	14·70	$\bar{2}01$	Plagioclase
22·55	3·978	14·70		Plagioclase
22·97	3·870	14·70	$1\bar{1}1$	Plagioclase
23·65	3·762	15·68		Analcite–Plagioclase
23·80	3·739	14·70		Plagioclase
24·15	3·685	19·60		Analcite–Plagioclase
25·10	3·547	21·56		Plagioclase
25·55	3·487	18·62		Plagioclase
25·90	3·440	15·68		Plagioclase
26·65	3·345	42·14		Plagioclase
26·85	3·321	24·50		Plagioclase
27·50	3·244	40·18		Plagioclase
27·95	3·192	100·00		Plagioclase
28·70	3·110	15·68	220	Plagioclase
29·25	3·053	13·72		Plagioclase
29·65	3·013	17·64		Plagioclase–Analcite
29·90	2·988	20·58	$1\bar{3}1$	Plagioclase
30·35	2·942	17·64		Plagioclase
30·75	2·905	17·64		Plagioclase
31·35	2·854	16·66		Analcite
31·70	2·820	14·70	131	Plagioclase
32·15	2·785	13·72		Analcite

Table 6. X-ray diffraction data of the light fraction of Sample no. 5

2θ	dA°	I/Io	hKL	Corresponding mineral phase
20·85	4·260	18·87		Quartz
21·10	4·210	15·10		Plagioclase
21·80	4·076	11·32		Plagioclase
22·00	4·050	18·87	$\bar{2}01$	Plagioclase
22·20	4·005	12·27		Plagioclase
22·45	3·960	13·21		Plagioclase
22·85	3·892	12·27	$1\bar{1}1$	Plagioclase
23·25	3·826	16·04		Plagioclase
23·75	3·747	18·87		Plagioclase
24·20	3·678	26·42		Plagioclase
24·85	3·583	11·32		Plagioclase
25·50	3·464	18·87		Plagioclase
26·15	3·408	13·21		Plagioclase
26·65	3·345	49·06		Plagioclase
27·05	3·297	22·64		Analcite
27·20	3·279	18·87		Plagioclase
27·55	3·238	69·82		Plagioclase
27·95	3·192	100·00		Plagioclase
28·20	3·164	33·02	220	Plagioclase
29·50	3·027	11·32	$1\bar{3}1$	Plagioclase
30·15	2·965	16·98		Plagioclase
30·35	2·946	18·87		Analcite
30·75	2·905	15·10		Plagioclase
31·45	2·845	16·04	131	Plagioclase
32·23	2·778	13·21		Analcite
32·80	2·731	13·21		Analcite

Table 7. X-ray diffraction data of the light fraction of Sample no. 6

2θ	dA°	I/Io	hKL	Corresponding mineral phase
22·30	3·988	22·22	$\bar{2}01$	Plagioclase
22·50	3·951	14·82		Plagioclase
23·15	3·843	14·82	$1\bar{1}1$	Plagioclase
23·65	3·761	13·89		Plagioclase
24·25	3·670	20·37		Plagioclase
24·50	3·634	18·52		Plagioclase–Analcite
25·36	3·514	40·74		Plagioclase
25·60	3·480	16·67		Plagioclase
26·35	3·380	14·82		Plagioclase
26·45	3·370	18·52		Plagioclase
26·75	3·333	25·93		Plagioclase
27·20	3·279	18·52		Plagioclase
27·65	3·226	22·22		Plagioclase–Analcite
28·15	3·170	100·00		Plagioclase
28·55	3·126	29·63		Plagioclase
29·45	3·033	14·82	220	Plagioclase
30·30	2·950	14·82	$1\bar{3}1$	Plagioclase
30·75	2·905	18·52		Plagioclase
30·95	2·889	14·82		Plagioclase
31·60	2·831	17·59		Plagioclase
31·80	2·805	14·82	131	Plagioclase
32·35	2·768	12·96		Analcite
33·10	2·706	12·96		Analcite
33·45	2·679	16·67		Analcite–Plagioclase

Table 8. Γ and β values for plagioclase feldspars in Abu Dob andesites

Sample no.	$\Gamma°$	$\beta°$
1	0·50	0·88
2	0·45	0·83
3	0·64	0·88
4	0·60	0·87
5	0·65	0·85
6	0·65	0·85

دراسة بتروجرافية ومعدنية لبعض قواطع الانديزيت بمنطقة أبو دب بالصحراء الشرقية المصرية

أحمد محمد بشادى
معهد التربية للمعلمين بالعديلية ،
الكويت

محمد عزالدين حلمى
قسم الجيولوجيا بكلية العلوم ،
جامعة عين شمس ، القاهرة

محمود لطفى كابش
مختبر علوم الارض بالمركز القومى للبحوث ،
الدقى ، القاهرة

خلاصة

لقد درست قواطع الانديزيت التى تخترق الصخور الجرانيتية بمنطقة أبو دب بالصحراء الشرقية المصرية . وقد كشفت الدراسة البتروجرافية للقطاعات الرقيقة في الصخور عن الانواع التالية : بلاجيوكليز ـ هورنبلند بورفير انديزيت ، بلاجيوكليز ـ بيوتيت ـ هورنبلند انديزيت بورفيرى ، كوارتز أنديزيت بورفيرى ، بلاجيوكليز ـ هورنبلند أنديزيت ، بايروكسين ـ هورنبلند أنديزيت .

ولقد أوضحت قياسات الاشعة السينية للبلاجيوكليز المفصول من ستة من الانديزيت البورفيرى ان الحالة البنائية لتلك البلاجيوكليزات هى حالة انتظام متوسط ، وهذا يساير تماما انتظام الصخور النارية الوسطية .

J. Univ. Kuwait (Sci.) **6,** 1979

Petrographical and petrochemical characters of some basalt dykes, Gebel Abu Dob area, Eastern Desert, Egypt

AHMED M. BISHADY AND MAHMOUD L. KABESH
Teachers' Institute of Education, El-Odylia, Kuwait and Earth Sciences Laboratory, National Research Centre, Dokki, Cairo, Egypt

ABSTRACT

Basalt dykes dissecting the granitic complex of Gebel Abu Dob, Eastern Desert, Egypt, are examined. Petrographic study of these dykes revealed the following varieties: pyroxene-hornblende basalt, hornblende basalt, biotite-hornblende basalt, quartz-bearing basalt and olivine basalt. Major element chemistry of 15 basalt dykes is presented and discussed. Petrochemically, the examined basalts are high in Al and belong to the tholeiitic series. Classification of the basalt dykes is attempted, using various schemes which comprise modal analysis, chemical composition, norm values, Kuno's S.I. and Kushiro and Kuno's relations.

INTRODUCTION

The present study deals with the petrography and petrochemistry of some basaltic dykes dissecting the granitic complex of Gebel Abu Dob, Central Eastern Desert, Egypt (Fig. 1).

The present work has been focussed on the following: (1) petrographic description of the basalt dykes, (2) evaluation of the major element chemistry of these dyke rocks, (3) an attempt to classify the examined dykes using different schemes of classification.

The dominant trends of these dykes are NS and NE–SW. The majority tend to form parallel swarms, which are either vertical or steeply inclined at angles of 70–85°. The basalt dykes are generally less resistant to weathering than the host granites. They may be weathered into cuboidal onion-like boulders.

PETROGRAPHY

The basaltic dykes in Abu Dob exhibit a dominant even-grained texture. Porphyritic basalts and porphyries are less common. Other textures are the ophitic to subophitic and subtrachytic. Of particular interest is the frequent presence of amygdales, giving rise to amygdaloidal basalts. Such amygdales reach up to 7·7 mm across and are oval to rounded. They may be filled with successive layers of chlorite, epidote, zoisite and carbonates. Examination of thin sections gave the following mineralogical varieties: pyroxene-hornblende basalt, hornblende basalt, biotite-hornblende basalt, quartz-bearing basalt and olivine basalt.

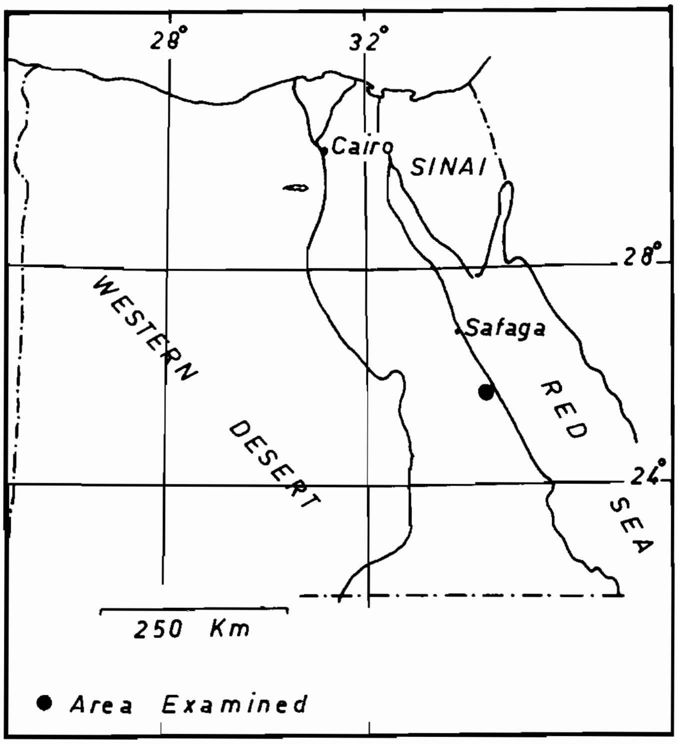

Fig. 1. Location map.

Mineral description. Plagioclases exist as small crystals of groundmass dimension down to lath-shaped microlites. The megacrysts vary in length from 5·5 to 0·9 mm and in breadth from 0·5 to 0·2 mm. Prismatic plagioclases in the groundmass reach up to 0·8 mm in length and 0·25 mm in breadth. Megacrysts usually have fresh cores and altered rims, and are occasionally corroded showing ragged and embayed outlines. Such irregular outlines are possibly due to magmatic corrosion. In addition to lamellar, Carlsbad or combined Albite–Carlsbad twinning, the cross and T form (Banatar type) are observed. The average composition of the megacrysts is about An_{55} (labradorite), but in the groundmass it is about An_{50}. Although plagioclases occur in more than one generation, the variation in composition between the megacrysts and groundmass plagioclases does not permit a sharp line of demarcation to be drawn between them. Alteration ranges from moderate to intense and comprises epidote, zoisite, carbonate, and chlorite.

Hornblende forms megacrysts varying from 1·2 to 0·6 mm in length and from 0·8 to 0·2 mm in breadth. Small prismatic crystals of hornblende in the groundmass attain up to 0·6 mm in length and 0·1 mm in breadth. Hornblende megacrysts may be completely pseudomorphed by iron oxides or chlorite. They are strongly pleochroic with green and brown colors. Green varieties are more common than browns and have $z \wedge c$ from $-10°$ to $-13°$. In the groundmass, hornblende is rather fresh brown or green in colour. Due to possible oxidation of the green variety, both types are observed in common association.

Pyroxenes are represented by augite, diopsidic augite and pigeonitic augite. They occur as subhedral to anhedral grains attaining up to 1·3 mm in length and 0·9 mm in breadth. They do not exist as megacrysts. The measured optic axial angle (2V) averages 45°. Occasionally they exhibit simple twinning and hour-glass structure.

Biotite occurs only in the groundmass forming irregular flakes with ragged ends reaching up to 0·6 mm in length and 0·12 mm in breadth. Flakes are strongly pleochroic with X = straw yellow and Y = Z = chestnut brown. Some of the biotite is the result of alteration of hornblende.

Olivine is rarely encountered and is usually altered along fractures into serpentinous material.

The examined basalts comprise the following accessories: iron oxides as magnetite, hematite and grains of chromite which form subhedral to subrounded grains attaining up to 0·4 mm across. Quartz, apatite, rutile, sphene and glass are also observed as accessories.

The most common alteration products are chlorite, epidote, iron oxides and carbonates. It is argued that some of these alteration products are possibly due to some late stage (deuteric) action. This may be supported by the observation that the amygdales are filled with secondary minerals of which the most typical are chlorite, carbonates, epidote, zeolites, silica minerals and serpentine.

Modal composition. The quantitative mineral composition for 14 representative samples of the basalt dykes is given in Table 1. It is evident from the modes that phenocrysts in the examined porphyritic basalts and basalt porphyries show a wide range from 9·7% to 21·5%. Plagioclase phenocrysts represent the dominant type. Hornblende megacrysts range from 3·9% to 4·2%.

The colour index, representing the sum of mafic minerals (hornblende + pyroxene + olivine), plus accessories and alteration products, calculated for the examined basaltic dykes (Table 1) is rather high and ranges from 37·6% to 92·2%. These high values may be due to the fact that all the alteration products were considered as mafic minerals. Thus Abu Dob basalts are mesocratic to melanocratic according to Streckeisen (1967).

PETROCHEMISTRY

Data for chemical analysis are given in Table 2. SiO_2, MgO and R_2O_3 group (Al_2O_3 + total iron + TiO_2) were determined gravimetrically. Total iron and TiO_2 were estimated colorimetrically and Al_2O_3 determined by subtraction. FeO was estimated by titration against standard solution of potassium permanganate, and Fe_2O_3 was determined by subtraction of FeO from total iron. Na_2O, K_2O and CaO were determined by flame photometry. P_2O_5 and MnO were determined colorimetrically. Their petrochemical interpretations are as follows:

Major elements. Ternary plot of alkalis ($Na_2O + K_2O$)—MgO—($FeO + 0{\cdot}9Fe_2O_3$), shows that the examined basalts are rich in iron and relatively rich in magnesia at the expense of alkalis (FAM diagram, Fig. 2a). They are also enriched in CaO at the expense of K_2O and Na_2O, which is evident from the ternary plot of K_2O—CaO—Na_2O (KCN diagram, Fig. 2b). The differentiation of the basaltic magma broadly involves the fractional crystallisation of the two contrasted mineral groups, the mafic (olivine, pyroxene, amphiboles and biotite) and the felsic (chiefly feldspars). Simpson (1954, p. 238) attempted to assess the relative evidence of the two mineral groups upon

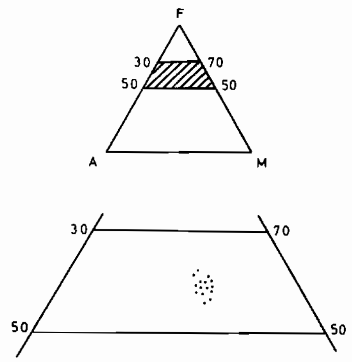

Fig. 2a. FAM diagram of Abu Dob basalt: F = $FeO + 0{\cdot}9Fe_2O_3$; M = MgO; A = $Na_2O + K_2O$ (in wt.%).

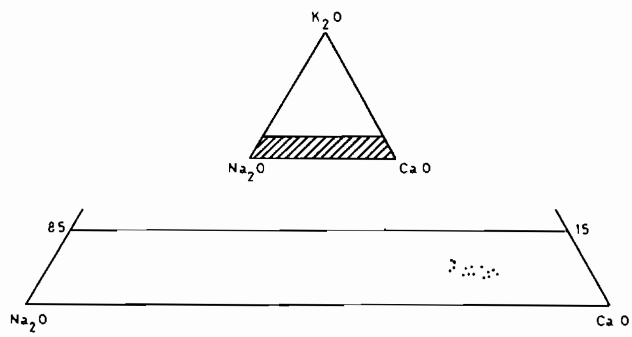

Fig. 2b. CaO—K_2O—Na_2O diagram.

the differentiation trend of basic magma. He stated that the felsic minerals (chiefly feldspars) constitute Bowen's continuous reaction series, which experimental work has shown to be enriched in alkalis at the expense of lime during fractional crystallization. The ratio

$$\frac{Na_2O + K_2O}{Na_2O + K_2O + CaO} \times 100$$

provides a convenient index of the degree of fractionation of felsic minerals and the term'felsic index' (F) has been proposed by Simpson (1954). On the other hand the mafic group (olivine, pyroxene, amphiboles and biotite) corresponds to Bowen's discontinuous reaction series, yet each individual mineral series within this group constitutes a continuous reaction series in which fractional crystallisation leads to iron enrichment at the expense of Mg. The ratio

$$\frac{FeO + Fe_2O_3}{MgO + FeO + Fe_2O_3} \times 100$$

which was devised by Wager & Deer (1939) may be used as index of mafic fractionation and has been designated 'mafic index' (M) by Simpson (1954).

The felsic index (F) and mafic index (M) for the examined basalts are given in Table 2,

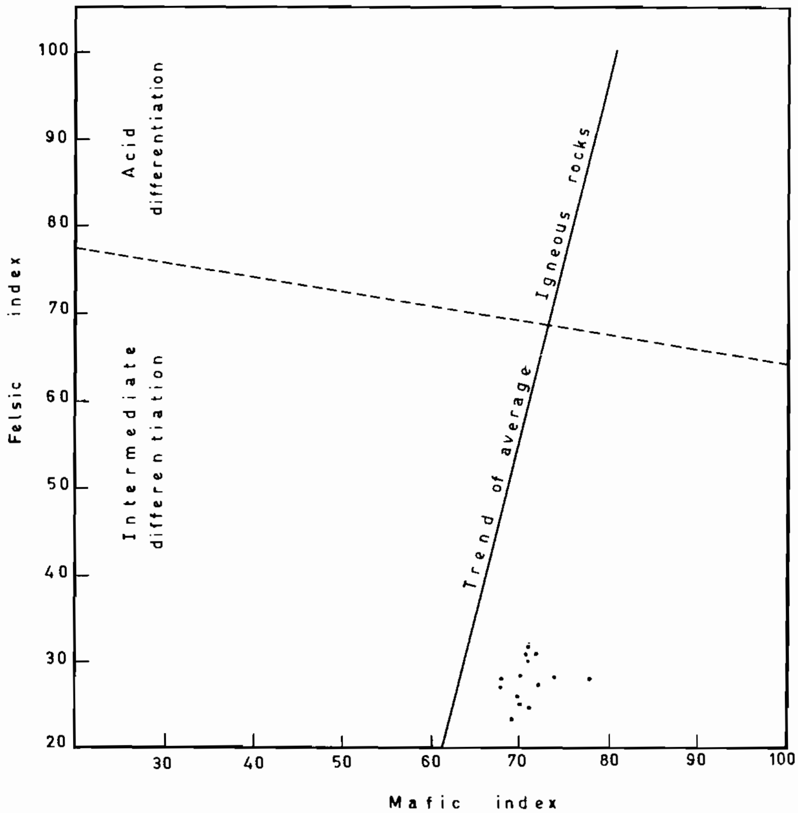

Fig. 3. Plot of mafic vs. felsic indices for Abu Dob basalt. The solid line represents Nockolds' trend of average igneous rocks (Nockolds 1954).

and the relation between the two indices are plotted (Fig. 3). The diagram is roughly divided into two fields, a lower one for intermediate differentiation and an upper one for acid differentiation. Fig. 3 shows that all the examined basalts are located below the lowermost limit (40) for felsic index as given by Nockolds (1954). All the examined basalts possess high mafic index.

Alkali ratios. Values of the alkali ratio for the examined basalts are given in Table 3. It is clear that the alkali ratio is rather consistent in the majority of these basalts with an average K_2O/Na_2O ratio of 24·33. This shows that the basalts are clearly sodic. Generally the potash/soda ratio is distinctly less than 0·4 with an average of 0·32.

The serial characters. The σ values (Rittmann's suite index) are calculated for the basaltic dykes and presented in Table 4. They range from 1 to 3 with an average of 2·22.

The T value

$$\frac{Al_2O_3 - Na_2O}{TiO_2} \text{ (wt\%)}$$

(Table 4) has been considered a solid indicator for the distinction of simatic and sialic material (Rittmann 1967). It is clear from Fig. 4 that the examined basalts have T values

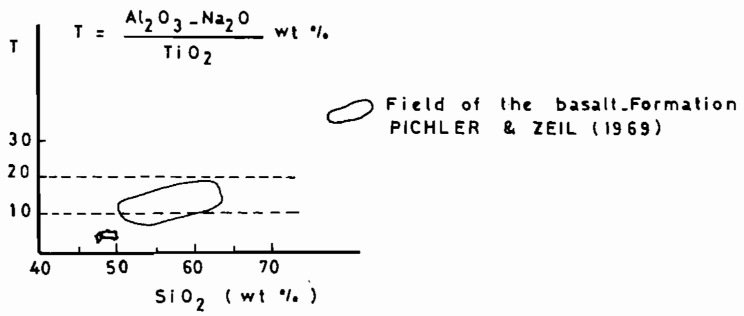

Fig. 4. *T*-Values vs. SiO_2.

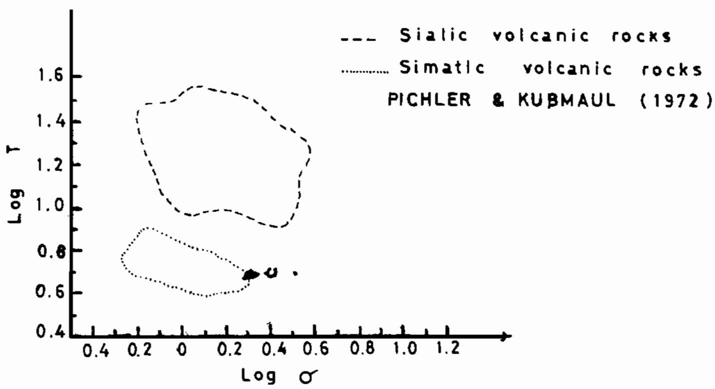

Fig. 5. Log σ vs. log *T* diagram.

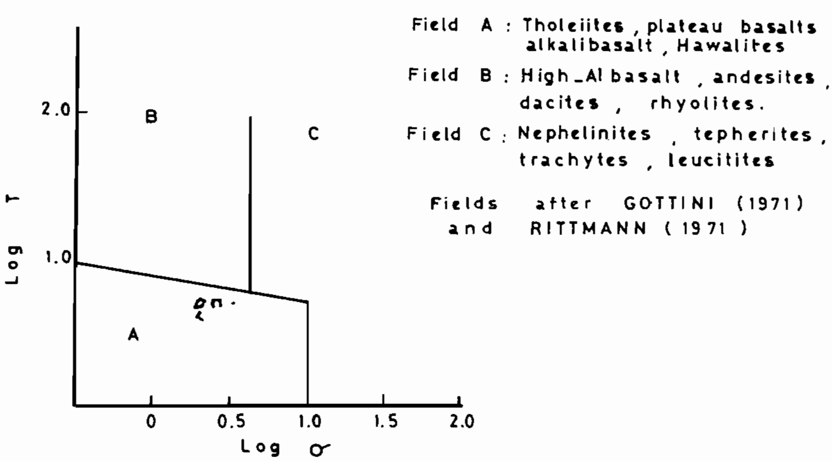

Fig. 6. Log σ vs. log *T* diagram.

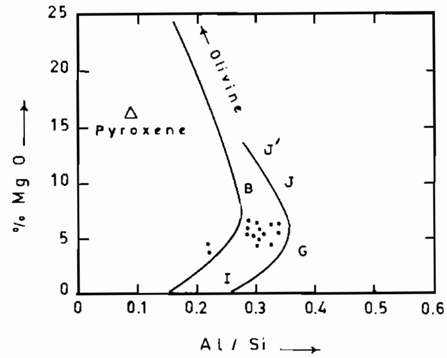

Fig. 7. Variation diagram for MgO (wt.%) vs. Al/Si ratio. Fields after Murata (1960). B. Tholeiitic basalt; G, Hawaiite (andesine andesite); I, Trachyte; J–J, Alkalic (olivine) basalt.

less than 10, pointing to their possible simatic character. It is also clear from (Fig. 5) that the examined basalts plot very close to the field representing simatic volcanic rocks (Pichler & Kußmaul 1971), while Fig. 6 also shows that all the examined basaltic dykes plot within Field A given by Rittmann (1971), Gottini (1971) and Negendank (1972) for basalts. The plotting of MgO% against the weight percentage ratio of Al_2O_3/SiO_2 (Murata 1960) is presented in Table 3 and shows that all the basalts examined plot very close to 'B' (tholeiitic basalt) and 'C' (quartz basalt) (Fig. 7).

Norm values. Niggli's molecular norms of the analysed basalts are calculated according to Barth (1962) and presented in Table 5. The distribution of the normative feldspars recalculated to 100% (Table 6) is projected in the Or–Ab–An ternary diagram (Fig. 8). It is evident that the basalts examined plot close to the Ab–An side far away from the Or apex. Also, from this diagram it is clear that the normative composition of the feldspars of these basalts varies between An_{43} to An_{53}.

The calculated norm includes up to 5·8% Or. Yoder & Tilley (1962) stated that most basalts contain less than 1% K_2O and broadly speaking this gives at most 5·9% Or. This supports the results given in the present work.

The plotting of the normative pyroxenes calculated to 100% in the ternary diagram Wo–En–Fs is shown in Fig. 9, in which the subdivisions are made after Deer *et al.*

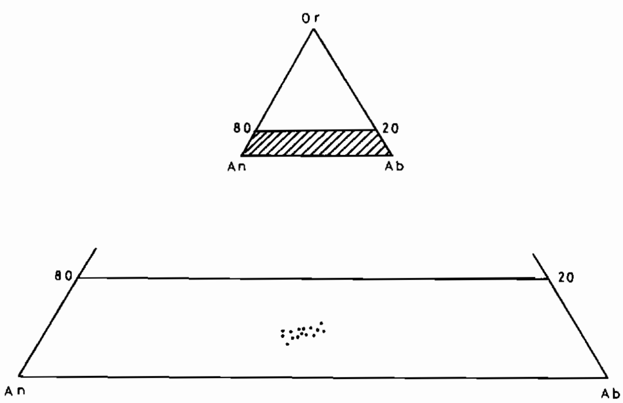

Fig. 8. Normative Or–Ab–An diagram.

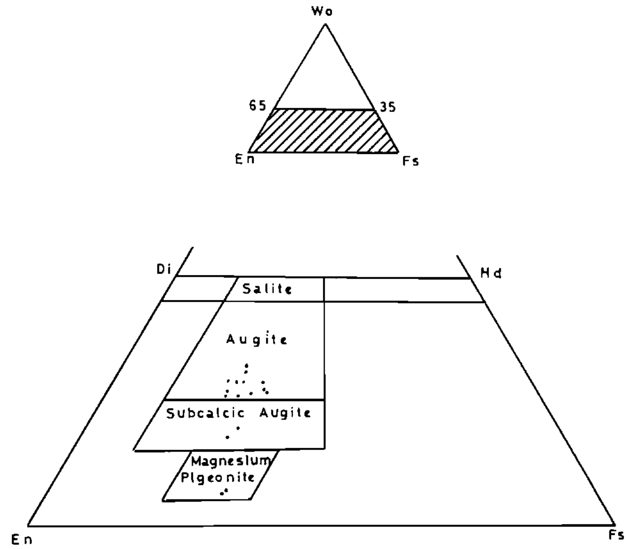

Fig. 9. Wo–En–Fs diagram.

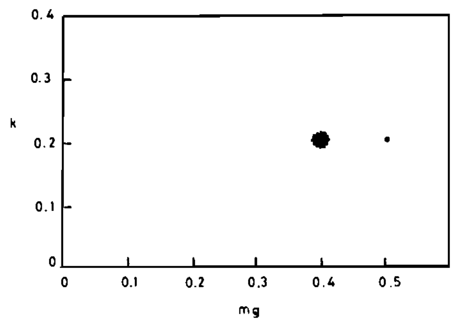

Fig. 10. Relation of mg and k values of Niggli.

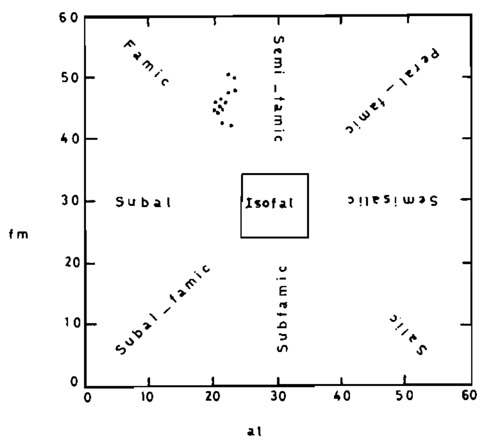

Fig. 11. Relationship of al and fm (after Burri & Niggli 1945).

(1966).The diagram shows that the pyroxenes of the examined basaltic dykes plot in the fields of augite, subcalcic augite and Mg-augite. It is also evident that the composition of the normative pyroxenes lies well below the Di–Hd line which is typical of the composition of pyroxenes occurring in calc alkaline rocks.

Niggli values. The calculated Niggli values (Barth 1962) for the examined basaltic dykes are given in Table 7. The relationship between (k–mg) values (Fig. 10) shows that all values of k are 0·2, and the mg values are higher than 0·4. This means that the examined basalts are characterised by slight mg tendency. Also the values of al are plotted against fm values of Niggli (Fig. 11). These relations show that the character of the magma is femic to semifemic, according to Burri and Niggli's classification (1945).

CLASSIFICATION

The values of Kuno's solidification index, S.I. (Kuno 1959) for the examined basaltic

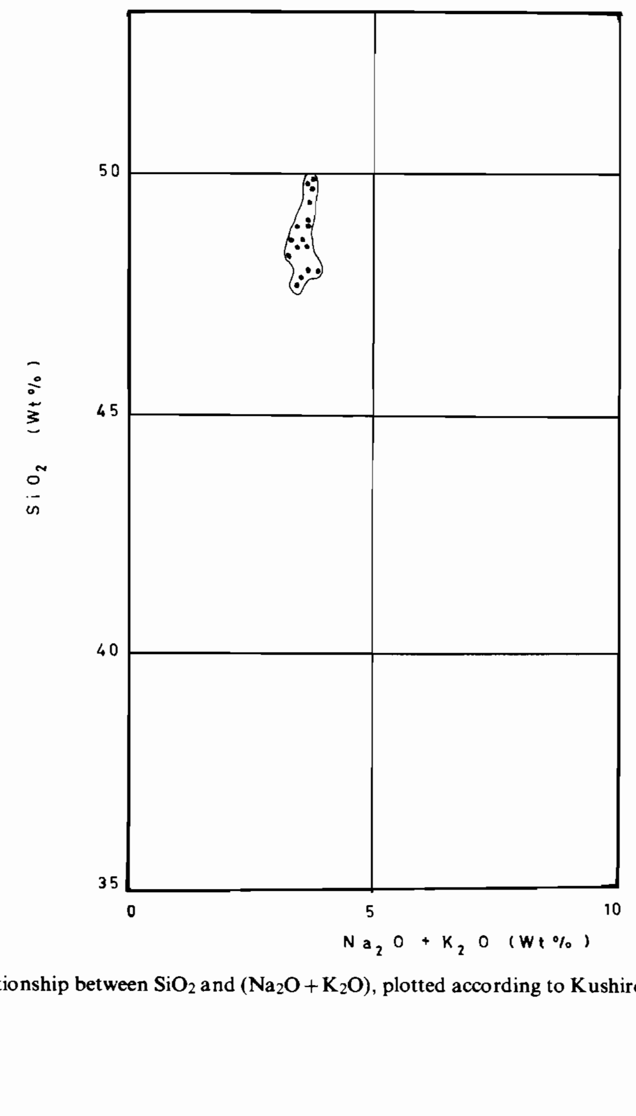

Fig. 12. The relationship between SiO_2 and (Na_2O+K_2O), plotted according to Kushiro & Kuno (1963).

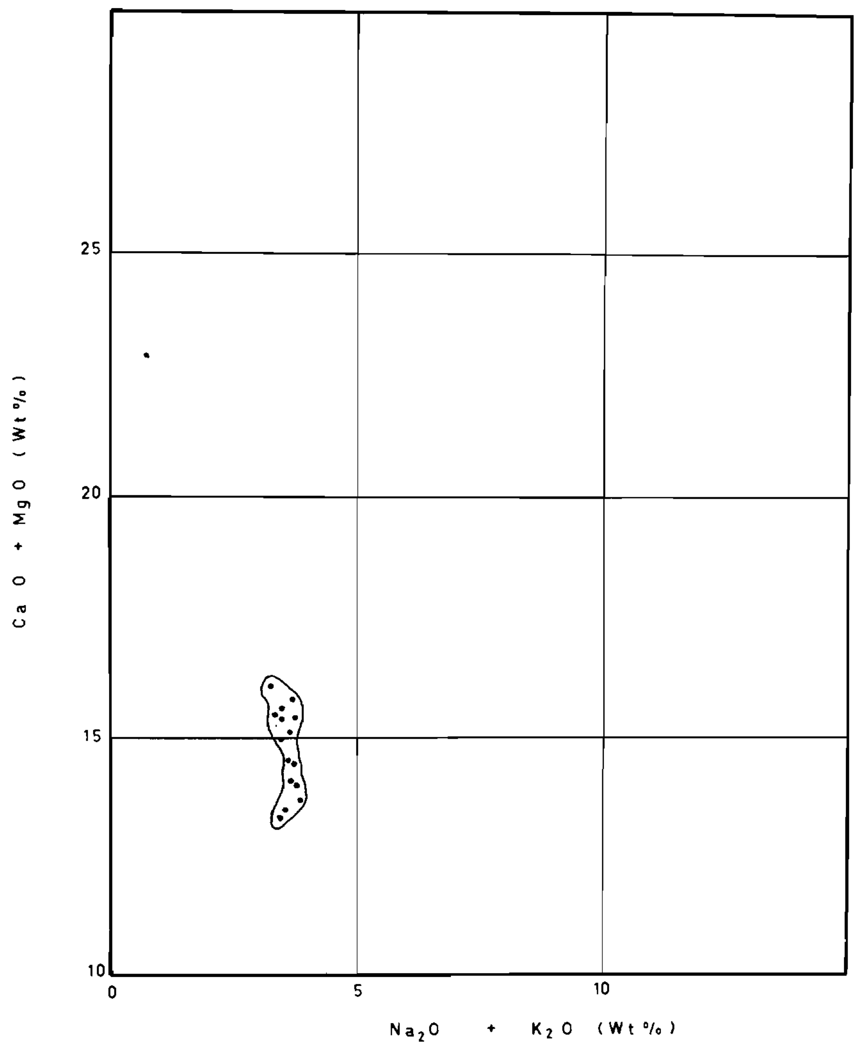

Fig. 13. Relationship between (CaO + MgO) and ($Na_2O + K_2O$), plotted according to Kushiro & Kuno (1963).

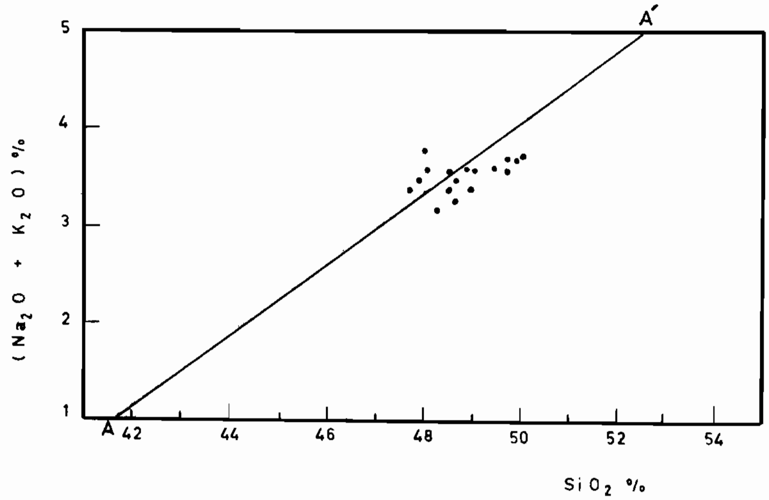

Fig. 14. Relationship between (Na_2O+K_2O) and SiO_2, plotted according to MacDonald & Katsura (1964).

dykes are given in Table 8. Since they have an average value of 24·31, it appears that the examined basalts possess andesitic tendencies.

Kushiro & Kuno (1963) advanced a classification of basalts by plotting SiO_2 vs. (Na_2O+K_2O) and ($MgO+CaO$) vs. (Na_2O+K_2O), all in wt%. Plotting of SiO_2 vs. alkalis is presented in Fig. 12. It shows that all the basalts examined fall in the group which includes all tholeiitic and high alumina basalts (Kushiro & Kuno 1963, p. 81). From the plotting of alkalis vs. ($CaO+MgO$), all in wt% (Fig. 13), it is evident that all the basalts examined fall in the area of the tholeiitic series (Kushiro & Kuno 1963, p. 82).

Following MacDonald & Katsura (1964), the total alkalis are plotted vs. SiO_2, all in wt% (Fig. 14). The majority of these basaltic rocks fall close to the line AA′. Thus

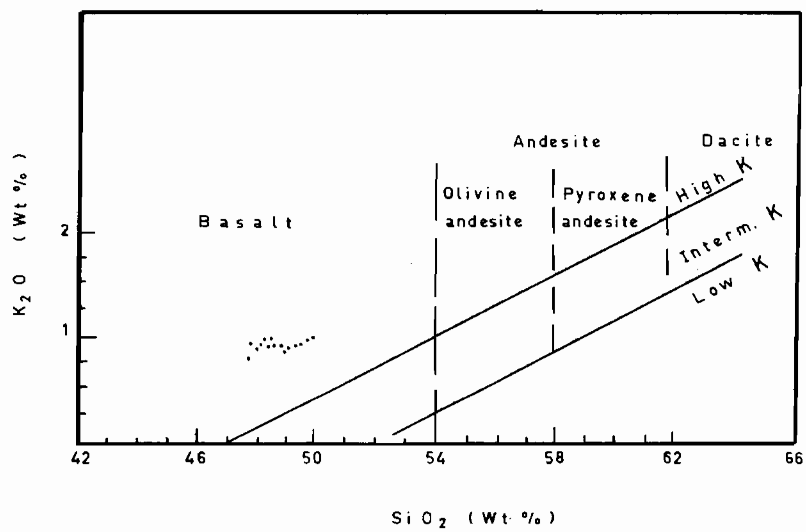

Fig. 15. Chemical classification of basalts (K_2O vs. SiO_2).

they belong to the normal tholeiitic basalts. Plotting of SiO_2 vs. K_2O (Fig. 15) shows that the examined basalts all fall very closely in the area of basalt with high K.

Normative classification. Yoder & Tilley (1962) made use of the calculated normative components of basalts and divided them into five groups. According to this classification, and from the normative values of the examined basalts (Table 5), they appear to belong to the saturated tholeiitic types.

REFERENCES

Barth, T.F.W. 1962. Theoretical petrology. John Wiley.

Burri, C. & Niggli, P. 1945. Die jungen Eruptivgesteine des mediterranean Orogens, 1. Pupl. Vulkaninstitut Immanuel Friedländer No. 3, Zurich.

Deer, W.A., Howie, R.A. & Zussmann, J. 1966. An introduction to the rock-forming minerals. Longmans, London.

Gottini, V. 1971. Some remarks on contact anatexis. Bull. Volc. **34:** 406–13.

Kuno, H. 1959. Origin of Cenozoic petrographic provinces of Japan and surrounding areas. Bull. Volc. **20:** 37–76.

Kushiro, I. & Kuno, H. 1963. Origin of primary basalt magmas and classification of basaltic rocks. J. Petrology **4:** 75–89.

MacDonald, G.A. & Katsura, T. 1964. Chemical composition of Hawaiian Lavas. J. Petrology **5:** 82–133.

Murata, K.J. 1960. A new method of plotting chemical analyses of basalt rocks. Amer. J. Sci. **258:** 247–52.

Negendank, J.F.W. 1972. Volcanics of the valley of Mexico. Description of some Mexican volcanic rocks with special consideration of the opaques. N. Jb. Miner. Abh. **116:** 308–20.

Nockolds, S.R. 1954. Average chemical composition of igneous rocks. Bull. Geol. Soc. Amer. **65:** 1007–32.

Peacock, M.A. 1931. Classification of igneous rock series. J. Geol. **39:** 54–67.

Pichler, H. & Kußmaul, S. 1972. The calc-alkaline volcanic rocks of the Santorini group, Aegean sea, Greece. N.Jb. Miner. Abh. **116:** 268–307.

Pichler, H. & Zeil, W. 1969. Andesites of the Chilean Andes. In **McBirney, A.R. (Ed.)** Proceedings of the Andesite Conference. Oregon Dept. Geol. Mineral. Ind. Bull. **65:** 165–74.

Rittmann, A. 1957. On the serial character of igneous rocks. Egypt. Jour. Geol. **1:** 23–48.

Rittmann, A. 1967. Die Bimodalität des Vulkanismus und die Herkunft der Magmen. Geol. Rdsch. **57:** 277–295, Stuttgart.

Rittmann, A, 1971. The probable origin of high-alumina basalts. Bull. Volc. **34:** 414–20.

Simpson, E.S.W. 1954. On the graphical representation of differentiation trends of igneous rocks. Geol. Mag. **91:** 238–44.

Streckeisen, A. 1967. Classification and nomenclature of igneous rocks. N. Jb. Miner. Abh. **107:** 144–214.

Wager, L.R. & Deer, W.A. 1939. Geological investigations in East Greenland. Petrology of Skaergard Intrusion. Med. Om. Greenland **105:** 1–352.

Yoder, H.S. Jr. & Tilley, C. 1962. Origin of basalt magmas: an experimental study of natural and synthetic rock systems. J. Petrology **3:** 342–532.

(Received 8 October 1977)

Table 1. Modal analysis of basalt dykes* in Abu Dob area

	1	2	3	4	5	6	7	8	9	10	11	12	13	14
Megacrysts														
Plagioclase								9·7		21·5	4·4		10·1	
Hornblende									3·9				4·2	
Groundmass														
Plagioclase	45·9	41·0	41·1	40·6	45·1	30·9	49·4	37·4	41·6	37·6	47·0	33·3	42·2	7·8
Augite	6·1		9·8	5·2	14·0	2·7	3·7	8·9	2·1	2·2	1·7	12·2	2·2	5·6
Hornblende	1·8	16·5	5·9	1·0	9·9	32·0	8·6	2·3	10·9	9·7	9·3	28·4	7·7	4·2
Biotite						3·2				16·1	23·8		14·2	
Olivine														6·7
Quartz										3·2	1·7		4·2	
Accessories	19·3	16·2	7·9	19·1	14·5	8·3	14·9	13·2	7·4	8·6	6·8	4·3	5·2	20·1
Alteration products	23·3	26·4	35·4	34·1	16·5	22·6	23·4	28·5	34·1	1·1	5·5	21·8	10·0	55·6
Amygdales	3·7													
Total	100	100	100	100	100	100	100	100	100	100	100	100	100	100
Colour Index	54·1	59·0	58·9	59·4	54·9	69·1	50·6	52·9	58·4	37·6	47·0	66·7	43·5	92·2

* Data represent averages of 6 to 8 thin sections for every dyke. In each section 800–1,000 points were counted.

Table 2. Chemical analysis of Abu Dob basalts

	Sample no.														
	1	2	3	4	5	6	7	8	9	10	11	12	13	14	15
SiO_2	49·42	48·51	48·63	49·82	49·90	48·92	48·25	47·85	47·69	48·53	49·07	49·68	48·89	47·95	47·99
TiO_2	2·35	2·39	2·34	2·41	2·45	2·32	2·39	2·35	2·42	2·38	2·41	2·45	2·39	2·44	2·36
Al_2O_3	13·84	14·75	15·43	14·76	13·89	14·65	14·44	15·69	15·81	14·67	14·42	13·98	14·75	12·25	15·32
Fe_2O_3	4·81	3·92	3·89	3·95	4·41	4·52	4·36	5·09	4·93	4·63	4·25	4·13	4·35	4·89	4·81
FeO	8·79	7·83	7·71	8·10	8·76	8·22	8·12	9·11	9·21	7·91	7·88	7·92	8·21	8·76	8·72
MnO	0·73	0·68	0·69	0·70	0·62	0·66	0·79	0·82	0·66	0·76	0·73	0·82	0·76	0·71	0·79
MgO	4·62	4·96	4·86	4·73	4·57	5·20	5·46	5·85	5·72	5·41	5·62	5·74	5·32	5·58	5·33
CaO	9·48	10·79	10·59	9·78	9·48	10·36	10·66	7·68	7·59	9·94	9·43	9·93	9·22	8·47	8·39
Na_2O	2·81	2·71	2·68	2·75	2·74	2·58	2·32	2·64	2·68	2·45	2·76	2·78	2·83	2·81	2·82
K_2O	0·81	0·85	0·81	0·87	0·98	0·79	0·86	0·89	0·75	0·95	0·84	0·89	0·81	0·83	0·97
H_2O	1·21	1·30	1·14	0·89	0·92	0·66	1·11	0·70	1·36	1·15	1·30	0·89	1·15	1·12	1·45
P_2O_5	0·69	0·72	0·62	0·79	0·80	0·65	0·75	0·81	0·68	0·69	0·71	0·82	0·80	0·75	0·73
Total	99·56	99·41	99·48	99·55	99·52	99·53	99·51	99·48	99·50	99·47	99·42	99·45	99·43	99·56	99·68
Mafic index	74·64	70·32	70·47	71·81	74·24	71·01	69·18	70·82	71·20	69·86	68·34	68·23	70·25	70·98	71·74
Felsic index	27·63	24·81	23·35	27·01	28·18	24·54	22·98	31·21	31·13	25·49	27·63	26·99	28·28	30·06	31·12

Table 3. Major element ratios in Abu Dob basalts

Sample no.	Alkali ratio	K_2O/Na_2O	Al_2O_3/SiO_2
1	22·38	0·29	0·28
2	23·88	0·31	0·30
3	24·62	0·30	0·32
4	24·03	0·32	0·30
5	26·34	0·36	0·28
6	23·44	0·31	0·30
7	27·04	0·37	0·30
8	25·21	0·34	0·33
9	21·87	0·28	0·33
10	27·94	0·39	0·30
11	23·33	0·30	0·79
12	24·25	0·32	0·28
13	22·25	0·29	0·30
14	22·80	0·30	0·32
15	25·59	0·34	0·32
Average	24·33	0·32	0·30

Table 4. Serial indices in Abu Dob basalts

Sample no.	σ	Log σ	T	Log T
1	2·04	0·3096	4·69	0·6712
2	2·30	0·3617	5·04	0·7024
3	2·16	0·3345	5·25	0·7202
4	1·91	0·2833	4·98	0·6972
5	2·01	0·3032	4·55	0·6580
6	1·92	0·2833	5·20	0·7177
7	1·93	0·2856	5·07	0·7050
8	2·59	0·4133	5·55	0·7443
9	2·51	0·3997	5·43	0·7348
10	2·09	0·3201	5·13	0·7101
11	2·14	0·3304	4·84	0·6848
12	2·02	0·3054	4·57	0·6599
13	2·25	0·3522	4·99	0·6981
14	2·47	0·3927	5·10	0·7076
15	2·88	0·4594	5·30	0·7243
Average	2·22		5·10	

Table 5. Norm values of Abu Dob basalts

	Sample no.														
	1	2	3	4	5	6	7	8	9	10	11	12	13	14	15
Ap	3·55	4·55	1·24	1·86	1·86	1·55	1·55	1·06	1·55	1·55	1·55	1·25	1·86	1·55	1·55
Il	3·36	3·48	3·48	3·48	3·60	3·36	3·48	3·36	3·48	3·48	3·48	3·56	3·48	3·60	3·48
Or	5·22	5·22	5·22	5·22	5·80	4·64	3·22	5·22	4·64	5·8	5·22	5·22	5·22	5·22	5·8
Ab	26·10	25·52	24·94	25·52	25·52	24·36	21·46	24·94	24·94	23·2	26·1	26·1	26·68	26·1	26·1
An	23·78	26·78	28·71	26·68	23·78	27·26	27·84	28·92	30·16	27·26	25·23	24·7	26·1	27·84	27·55
Wo	8·15	9·67	8·89	7·19	7·77	8·62	8·77	1·73	1·66	7·69	7·46	8·58	7·39	4·44	4·99
Mt	5·22	4·35	4·18	4·35	4·52	4·87	4·70	5·57	5·39	5·05	4·70	4·52	4·70	4·39	5·22
Fs	7·31	6·26	6·15	6·73	7·54	6·81	6·50	7·60	7·77	5·92	6·03	5·72	6·61	6·96	7·08
En	13·34	14·27	14·04	13·57	13·11	14·36	15·65	16·82	16·47	15·54	16·12	15·54	15·31	16·01	15·31
Qz	4·39	2·65	2·50	5·30	7·69	3·87	3·87	3·22	2·29	2·99	3·69	4·62	2·97	2·65	2·50
C	—	—	—	—	—	—	—	—	—	—	—	—	—	—	—
Colour index	32·94	39·57	37·97	37·18	38·39	39·96	40·85	36·91	36·33	39·23	39·34	39·78	39·35	37·94	37·63

Table 6. Normative feldspar percentages of Abu Dob basalts

Sample no.	Or%	Ab%	An%
1	9·47	47·37	43·16
2	9·08	44·37	46·55
3	8·87	42·36	48·76
4	9·09	44·44	46·47
5	10·52	46·32	43·16
6	8·25	43·30	48·45
7	6·13	40·86	53·01
8	8·84	42·21	48·95
9	7·76	41·75	50·49
10	10·31	41·24	48·45
11	9·23	46·15	44·62
12	9·32	46·59	44·09
13	9·00	46·00	45·00
14	8·82	44·12	47·06
15	9·76	43·90	46·34
Average	8·97	44·06	46·97

Table 8. Kuno's S.I. for Abu Dob basalts

Sample no.	S.I.
1	21·15
2	24·47
3	24·36
4	23·19
5	21·30
6	24·40
7	25·85
8	24·81
9	24·56
10	25·34
11	26·32
12	26·18
13	24·72
14	24·40
15	23·62
Average	24·31

Table 7. Niggli values of Abu Dob basalts

	Sample no.														
	1	2	3	4	5	6	7	8	9	10	11	12	13	14	15
al	20·42	21·26	22·27	21·90	20·76	20·96	20·55	22·29	22·73	21·05	20·89	20·39	21·48	22·16	22·09
fm	46·10	42·82	42·18	43·81	45·19	44·83	45·30	50·36	50·00	45·76	46·22	45·24	46·07	47·56	47·72
c	25·38	28·12	27·88	26·28	25·80	26·93	27·50	19·83	19·79	25·88	24·89	26·34	24·30	22·30	22·09
alk	8·11	7·77	7·67	8·01	8·24	7·28	6·66	7·53	7·48	7·31	8·00	8·04	8·15	7·98	8·10
si	123·6	118·5	119·5	125·4	126·9	116·6	116·2	115·3	116·4	118·1	121·0	123·0	120·6	117·9	117·6
k	0·17	0·17	0·17	0·17	0·19	0·16	0·20	0·17	0·16	0·20	0·17	0·17	0·16	0·17	0·18
mg	0·37	0·42	0·42	0·40	0·38	0·42	0·43	0·42	0·42	0·43	0·45	0·44	0·42	0·43	0·41
qz	−9·87	−12·60	−11·21	−6·66	−6·09	−12·49	−10·43	−14·76	−13·50	−11·11	−14·96	−9·09	−12·01	−14·05	−14·73

الخواص البتروجرافية والبتروكيميائية
لبعض قواطع البازلت
بمنطقة جبل أبو دب بالصحراء الشرقية المصرية

أحمد محمد بشادى
معهد التربية للمعلمين بالعديلية ،
الكويت

محمود لطفى كابش
مختبر علوم الارض بالمركز القومى
للبحوث ، الدقى ،القاهرة

خلاصة

اهتم البحث بدراسة قواطع البازلت التى تخترق الصخور الجرانيتية في منطقة جبل أبو دب بالصحراء الشرقية المصرية . ولقد كشفت الدراسة البتروجرافية لها عن وجود الانواع التالية : بايروكسين ـ هورنبلند بازلت ، بيوتيت هورنبلند بازلت ، بازلت حامل للكوارتز ، اوليڤين بازلت .

وتم عمل التحاليل الكيميائية للعناصر الشائعة في خمس عشرة عينة من قواطع البازلت ، ودرست هذه النتائج حيث دلت الدراسة البتروكيميائية على أن هذا البازلت كلسى الى كلسى الكيلى (باسيفى قوى الى باسيفى متوسط) ، وأن هذا البازلت به نسبة عالية من الالومينا وينتمى الى السلسلة الثيوليتية . وقد بذلت محاولات للتقسيم معتمدة على نظم مختلفة مثل حساب التكوين الفعلى ، والتركيب الكيميائى ، وحساب التكوين النموذجي ، ومعامل التجمد لكونو وعلاقات كوشيرو وكونو . ولقد أيدت هذه التقاسيم تماما نتائج الدراسة البتروكيميائية .